◆◆ Scientific
◆◆ Research

Synthesis and Characterization of Iron Oxide Nanoparticles Supported on Ziconia and Its Application in the Gas-Phase Oxidation of Cyclohexanol to Cyclohexanone

Mohammad Sadiq[1], Gul Zamin[1], Razia[1], Mohammad Ilyas[2]

[1]Department of Chemistry, University of Malakand, Chakdara, Dir (L), Khyber Pakhtunkhwa, Pakistan
[2]National Center of Excellence in Physical Chemistry, University of Peshawar, Khyber Pakhtunkhwa, Pakistan
Email: sadiq@uom.edu.pk, mohammad_sadiq26@yahoo.com

ABSTRACT

Iron oxide nanoparticles supported on zirconia were prepared by precipitation-deposition method and characterized by XRD, SEM, FT-IR, TGA/DTA, surface area and particle size analysis. Catalytic activities of the catalysts were tested in the gas-phase conversion of cyclohexanol in a fixed-bed flow type, Pyrex glass reactor, at 433 - 463 K. Major detected products were cyclohexanone, cyclohexene and benzene, depending on the used catalyst. The rate of reaction was significantly raised by the introduction of molecular oxygen in the feed gas, thereby suggesting the oxidation of cyclohexanol to cyclohexanone. Furthermore, the catalytic activity of iron oxide nanoparticles supported on zirconia treated with hydrogen at 553 K for 2 hours, was more selective and better than the unreduced iron oxide nanoparticles supported on zirconia, in the gas-phase oxidation of cyclohexanol to cyclohexanone. Experimental results showed that there was no leaching of metal, and that the catalyst was thus truly heterogeneous.

KEYWORDS

1. Introduction

Since the early 1900's, iron-based dispersed catalysts have been used for the liquification of coals. Continuous efforts have been made to reduce size of the particles with a simultaneous focus on preserving and enhancing the dispersion, in order to improve the quality and affordability of these iron-based catalysts. Several attempts have been made to prepare iron oxides and explore their catalytic activities in petrochemical industries [1-9]. Research has established the enhancing effect of promoters on the catalytic activity of iron-based catalysts, for example, molybdenum promotes the catalytic activity of sulfated hematite while tungsten has additive effect when used in combination with molybdenum. Similarly, nickel-cobalt has synergetic effect while used with molybdenum,

etc. [10-12]. Recently, researchers have diverted attention towards nano-materials and their applications in the field of catalysis. In this scenario, iron oxide nanoparticle is a potent candidate to be investigated as a catalyst in various industrially important reactions, including the synthesis of NH_3, water shift reaction, desulfurization of natural gas, dehydrogenation of ethyl benzene, oxidation of alcohol, and manufacture of butadiene [13-18].

In this work, we prepared iron oxide nanoparticles from iron nitrate with precipitating agents, *i.e.*, ammonium hydroxide and ammonium acetate, without the aid of any surfactant. Iron oxide particles were found to be in the range of 8 - 10 nm as estimated from XRD of pure iron oxide nanoparticles. Following the same procedure, iron oxide nanoparticles supported on zirconia were prepared by adding deionized water and monoclinic zirconia

to iron hydroxide prepared with ammonium hydroxide, or an excess of acetone and monoclinic zirconia to $Fe_2(CHOO)_6$ sol prepared with ammonium acetate. The prepared catalysts were characterized by various techniques, and tested for catalytic activities in the gas phase conversion of cyclohexanol to cyclohexanone, cyclohexene and benzene, keeping in view the fact that hematite and magnetite are semiconductors and can catalyze oxidation/reduction reactions [4].

2. Experimental

2.1. General

Chemicals were of high purity grade and were used as such without further purification. The catalyst was prepared in the laboratory from its precursor compounds. Nitrogen, oxygen and hydrogen were supplied by BOC Pakistan limited.

2.2. Catalyst Preparation

The catalyst was prepared in two steps.

2.2.1. Monoclinic Zirconia

Monoclinic zirconia was used as a support for the catalyst which was prepared by ammonolysis of $ZrOCl_2 \cdot 8H_2O$ (0.5 M aqueous solution) [19]. The precipitate was washed, dried, grinded, and then calcined at 1203 K in furnace at a rate of 1°C/min.

2.2.2. Fe_2O_3/Monoclinic ZrO_2

Fe_2O_3 nanoparticles were prepared by drop wise addition of

1) 0.5 M ammonium acetate solution to 0.1 M iron nitrate solution under vigorous stirring to obtain $Fe_2(CHOO)_6$ sol [16]. After the reaction, an excess of acetone and monoclinic zirconia were added and centrifuged to precipitate $Fe_2(OH)_6/ZrO_2$.

2) 0.5 M ammonium hydroxide solution to 0.1 M iron nitrate solution under vigorous stirring to obtain brownish precipitate. The precipitate was washed twice with triple distilled water and centrifuged. To the purified precipitates, deionized water and monoclinic zirconia were added and stirred, followed by centrifugation at 3000 rpm. Iron hydroxide/zirconia was then dried and calcined at 823 K which resulted in the nanoparticles of iron oxide supported on ZrO_2.

2.2.3. Reduction of the Catalyst

The prepared catalyst was reduced at 553 K in tube furnace for 2 h. The nitrogen gas was continuously passed through the reactor until the desired temperature (*i.e.*, 553 K) was achieved, and then a mixture of hydrogen and nitrogen (1:1) was passed for two hours at 40 mL/min, with a subsequent cooling in the nitrogen at-

mosphere.

2.3. Characterization of the Catalyst

Modern techniques such as XRD (X-ray differactrometer Rigaku D/Max-II, Cu tube, Japan), SEM (JSM 5910, JEOL, Japan), TGA/DTA (Diamond Series PerkinElmer, USA), U.K), FT-IR (Shimadzu prestige-21), Surface area and pore size analyzer (Quantachrome) were used for characterization of the catalyst.

2.4. Catalytic Test

100 mg of iron oxide nanoparticles supported on monoclinic ZrO_2 catalysts were used for the gas phase oxidation of cyclohexanol to cyclohexanone in a fixed-bed flow type Pyrex glass reactor at 433 - 463 K in a tubular furnace attached to temperature controller. Cyclohexanol vapors were fed from saturators, using N_2 as a carrier gas with a fixed flow rate of 40 mL/min. Reaction mixtures of 0.5 mL were injected at specified time intervals with six-port gas sampling valve to GC (PerkinElmer Clarus 580) with column (rtx@-Wax 30 m, 0.5 mm ID, 0.5 nm) and FID.

3. Results and Discussion

3.1. Characterization of the Catalyst

XRD of the catalysts, *i.e.*, one prepared with ammonium acetate and the other prepared with ammonium hydroxide as a precipitating agent, was carried out. XRD pattern of the former catalyst presented with peaks at $2\theta = 28.5$ and 31.8 which point towards a retention of the monoclinic phase of zirconia. However, the monoclinic phase of zirconia was lost in the latter catalyst which could probably be due to the presence of water. Furthermore, peaks at $2\theta = 35.4$ and 45.3 were recorded for both samples prior to being reduced, which account for the crystallized nanoparticles of iron oxide ($\alpha Fe_2O_3/\gamma Fe_2O_3$). In case of reduced samples, a peak was recorded at $2\theta = 69.2$ as shown in **Figure 1** which owes for the presence of magnetite in the samples [12,20,21].

The average particle size was estimated (8 - 10 nm) by using the Debye-Scherrer equation from peak width broadening in the XRD data of pure iron oxide (**Figure 2**). This finding is consistent with earlier studies of iron oxide nanoparticles [20,22].

BET surface area of the catalysts was found to be in the range of 150 - 300 m^2g^{-1}. FT-IR spectra (**Figure 3**) of freshly prepared sample exhibited peaks at 3300, 1642 and 1300 cm^{-1} corresponding to the O-H group, carboxyl group and NO_3^- ion, respectively [20,23]. But none of these peaks could be recorded for the unused calcined sample. However, peaks at 470 cm^{-1} and 570 cm^{-1} confirmed the presence of hematite particles in the unused calcined sample.
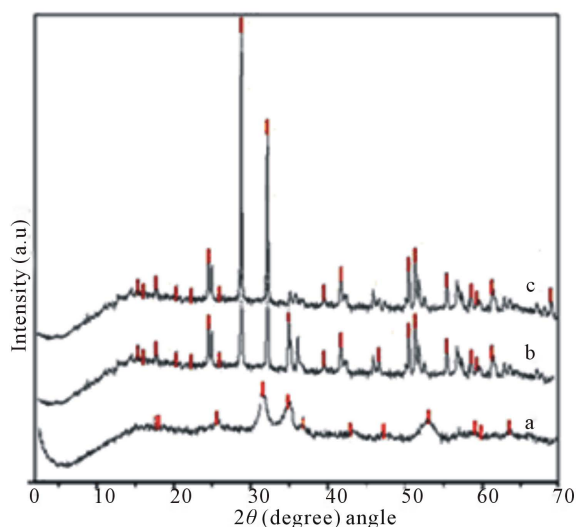
Figure 1. XRD patterns of the iron oxide nanoparticles supported on monoclinic zirconia: (a) Prepared with ammonium hydroxide as precipitating agent, and calcination at 823 K; (b) Prepared with ammonium acetate as precipitating agent, and calcination at 823 K; (c) Prepared with ammonium acetate as precipitating agent and calcination at 823 K, followed by reduction at 553 K in hydrogen flow for 2 hours.
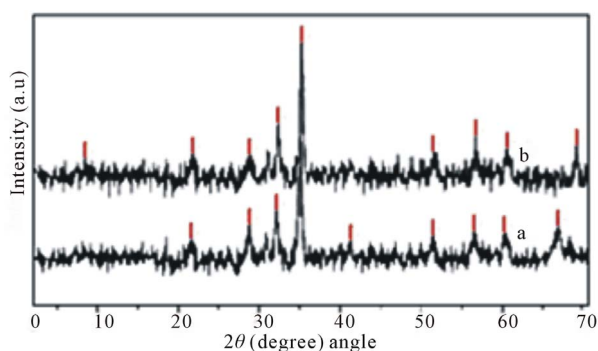
Figure 2. XRD patterns of the iron oxide nanoparticles: (a) Prepared with ammonium acetate as precipitating agent and calcination at 823 K; (b) Prepared with ammonium hydroxide as precipitating agent and calcination at 823 K, followed by reduction at 553 K in hydrogen flow for 2 hours.

SEM images (**Figure 4**) show that iron oxide nanoparticles prepared by using NH_4OH as precipitating agent are clustered together and bear a rough overall morphology, whereas those prepared by ammonium acetate as precipitating agent are well dispersed and have a smooth morphological presentation. SEM images clearly show that the morphological smoothness of the iron oxide nanoparticles in the latter sample enhances with calcination and reduction. After reduction in hydrogen flow, the nanoparticles appear as spherical balls. TGA/DTA study of freshly prepared dried catalysts, reflects a three stage reduction of iron oxide, and thereby strongly supports the procedure we have adopted for the preparation of hematite nanoparticles on monoclinic zirconia by calcination at 823
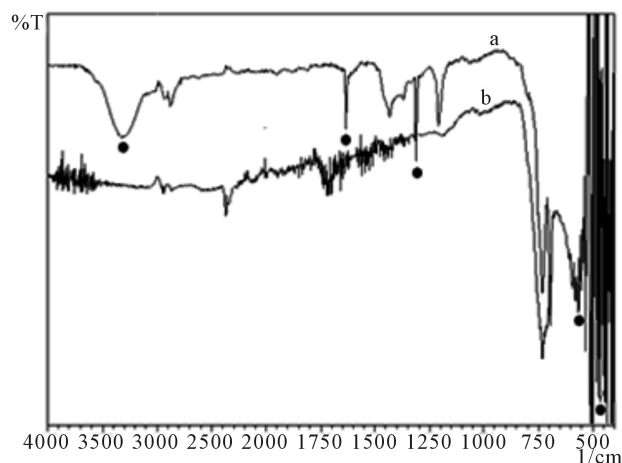
Figure 3. FT-IR of the iron oxide nanoparticles supported on monoclinic zirconia: (a) Before calcination, (b) After calcination.
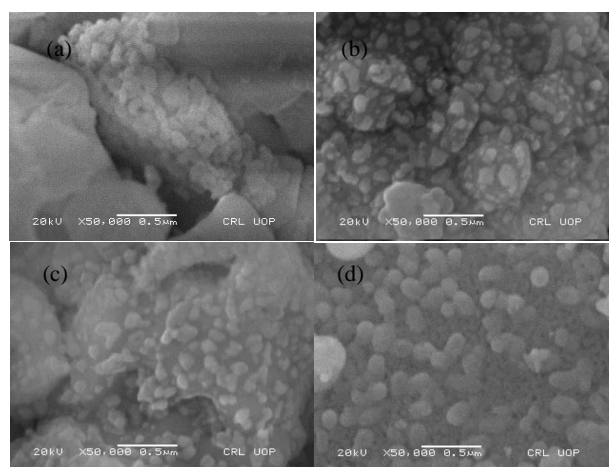
Figure 4. SEM images of iron nanoparticles on ZrO_2: (a) Prepared with ammonium hydroxide as precipitating agent; (b) Prepared with ammonium acetate as precipitating agent; (c) Prepared with ammonium acetate as precipitating agent and calcined; (d) Prepared with ammonium acetate as precipitating agent, calcined and reduced in hydrogen flow.

K, and for the preparation of magnetite nanoparticles on monoclinic zirconia by calcination at 823 K 4 hours followed by reduction at 553 K in hydrogen flow for 2 hours.

3.2. Oxidation/Dehydrogenation

Oxidation/dehydrogenation was demonstrated by comparing the data obtained with and without oxygen under identical experimental conditions using magnetite nanoparticles supported on zirconia as a catalyst as shown in **Figure 5**. A noticeable effect was observed on the rate of reaction, when oxygen (95 Torr) was introduced in the gas feeding system, in comparison to that obtained in pure N_2 atmosphere. The dehydrogenation activity falls again to the same negligible level when O_2 is removed

from the gaseous mixture. This increase in the rate of formation of cyclohexanone in the presence of O_2 is common for metal oxide catalysts and is known as oxidation. Most of the industrially important reactions proceed through oxidation pathway in the presence of metal oxide as catalysts.

The FT-IR spectra of the catalyst recovered from the reaction carried out in the oxygen flow using magnetite nanoparticles supported on zirconia showed intense peak for carbonyl group, thus showing that the major product of gas phase oxidation of cyclohexanol is cyclohexanone as shown in **Figure 6**. The percent yield calculated from FT-IR was in a good agreement with that of GC results.

The same reaction when carried out under identical condition using hematite nanoparticles supported on zirconia gives cyclohexene as a major product by dehydration of cyclohexanol as shown in FT-IR spectra (**Figure 7**). However with an increase in temperature, benzene was also detected suggesting digression of the reaction towards dehydrogenation as shown in **Scheme 1** [25-29].

3.3. Activation Energy

Variation in the rate of reaction with temperature at con-
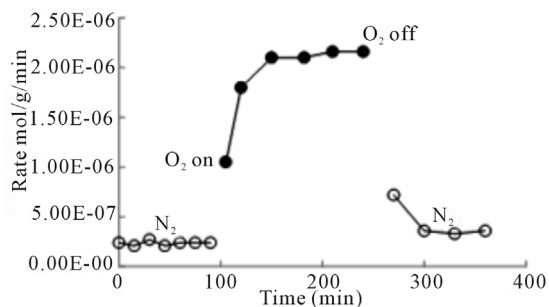
Figure 5. Activity profile of magnetite nanoparticles/monoclinic ZrO₂ for the conversion of cyclohexanol to cyclohexanone in an atmosphere of oxygen and nitrogen.
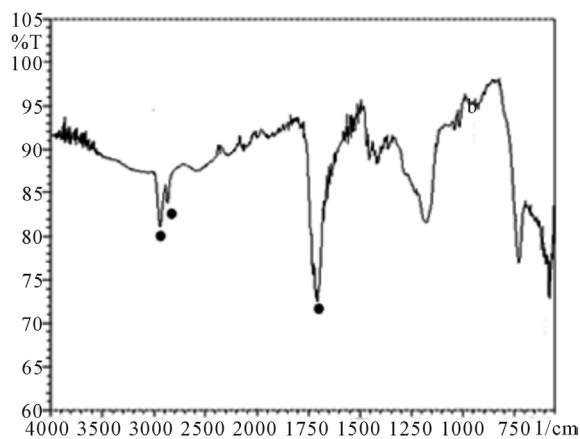
Figure 6. FT-IR of the recovered catalyst (magnetite nanoparticles supported on monoclinic zirconia), after being used for conversion of cyclohexanol.
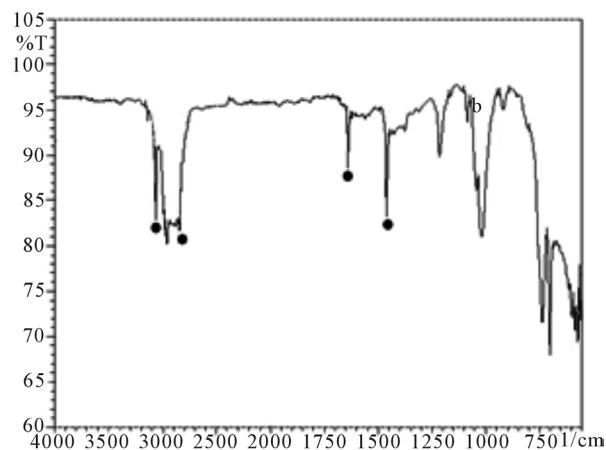
Figure 7. FT-IR of the recovered catalyst (hematite nanoparticles supported on monoclinic zirconia), after being used for conversion of cyclohexanol.
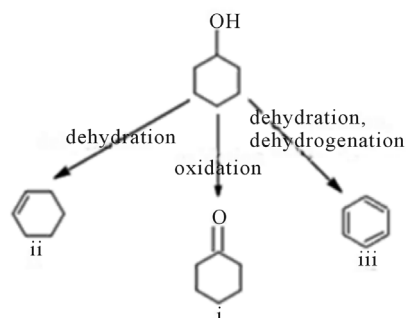
Scheme 1. Major products of cyclohexanol while using magnetite nanoparticles supported on monoclinic zirconia (i) or hematite nanoparticles supported on monoclinic zirconia (ii & iii).

stant pressures ranging from 12 Torr to 33 Torr was observed, using magnetite nanoparticles supported on monoclinic zirconia. Activation energies were calculated using Equation (4). Activation energies at pressures 12, 15, 20, 26, 33Torr are 17.48, 18.2, 17.73, 19.27, 19.73 kJ·mol^{-1}, respectively. The activation energies for all these pressures are in the range where reaction is diffusion controlled. The rate of a reaction is given by following equation.

$$\text{rate} = kP^n \tag{1}$$

According to Arrhenius equation

$$k = Ae^{-Ea/RT} \tag{2}$$

Putting the value of k from Equation (2) in Equation (1), we get

$$\text{rate} = Ae^{-\frac{Ea}{RT}}P^n \tag{3}$$

$$\ln \text{rate} = (\ln A + n\ln P) - Ea/RT \tag{4}$$

Plot ln rate vs. 1/T will give slope $= -Ea/RT$ while intercept $= \ln A + n\ln P$ as shown in **Figure 8**. Different

values of intercept as obtained from figure were plotted against $\ln P$ (**Figure 8**) where intercept = $\ln A$ and slope = n represent the order of reaction. The exposure of the catalyst in presence of oxygen was carried out for 480 minutes as shown in **Figure 9**. It is clear from the **Figure 9** that there is no noticeable decline in the catalyst activity.

4. Conclusion

The catalytic activity of hematite and magnetite nanoparticles supported on monoclinic zirconia was investigated for the gas-phase reaction of cyclohexanol. It was found that the catalyst was more active when reduced and selective for cyclohexanol oxidation to cyclohexanone, but it showed activity and selectivity for dehydration (*i.e.*, conversion of cyclohexanol to cyclohexene) when unreduced. Furthermore, the catalyst effectuated dehydration/dehydrogenation of cyclohexanol to benzene at higher temperatures. The model reaction, *i.e.*, the gas-phase oxidation of cyclohexanol to cyclohexanone using magnetite nanoparticles supported on monoclinic zirconia, in
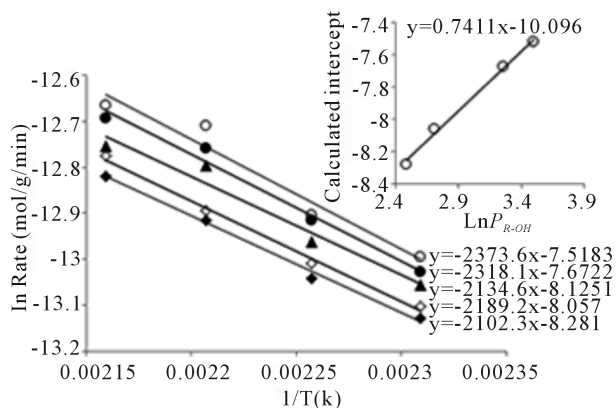
Figure 8. Plot of ln rate vs. 1/T (slope = $-Ea/RT$ and intercept = $\ln A + n\ln P_{ROH}$) and plot of $\ln P_{ROH}$ against calculated intercept.
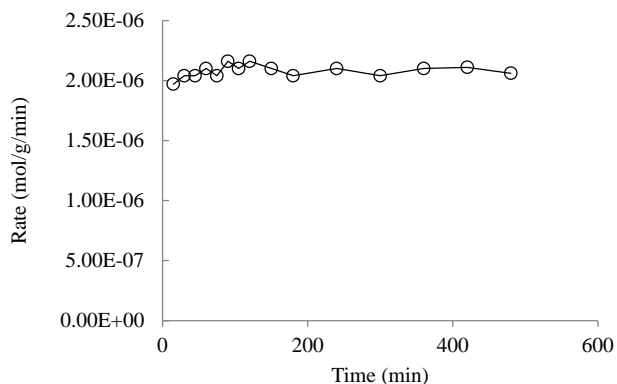
Figure 9. Continuous exposure of magnetite nanoparticles supported on monoclinic zirconia, used for conversion of cyclohexanol to cyclohexanone at 463 K.

flow reactor, was found to be in diffusion control regime. In addition, the iron oxide nanoparticles supported on monoclinic zirconia could be easily recovered and used several times without significant loss of catalytic activity.

Acknowledgements

REFERENCES

[1] R. M. Cornell and U. Schwertmann, "The Iron Oxides: Structure, Properties, Reactions, Occurrences and Uses," 2nd Edition, Wiley-VCH, Weinheim, 2003. http://dx.doi.org/10.1002/3527602097

[2] M. Azharuddin, H. Tsuda, S. Wu and E. Sasaoka, "Catalytic Decomposition of Biomass Tars with Iron Oxide Catalysts," *Fuel*, Vol. 87, No. 4-5, 2008, pp. 451-459. http://dx.doi.org/10.1016/j.fuel.2007.06.021

[3] C. Li, Y. Shen, M. Jia, S. Sheng, M. O. Adebajo and H. Zhu, "Catalytic Combustion of Formaldehyde on Gold/Iron-Oxide Catalysts," *Catalysis Communications*, Vol. 9, No. 3, 2008, pp. 355-361. http://dx.doi.org/10.1016/j.catcom.2007.06.020

[4] K. Choavarit, K. Tossapol, P. Phairat, C. Sumateand S. Ekasith, "Synergistic Activities of Magnetic Iron-Oxide Nanoparticles and Stabilizing Ligands Containing Ferrocene Moieties in Selective Oxidation of Benzyl Alcohol," *Catalysis Communications*, Vol. 26, 2012, pp. 1-5. http://dx.doi.org/10.1016/j.catcom.2012.04.016

[5] R. J. Zhang, J. J. Huang, H. T. Zhao, Z. Q. Sun and Y. Wang, "Sol-Gel Auto-Combustion Synthesis of Zinc Ferrite for Moderate Temperature Desulfurization," *Energy & Fuels*, Vol. 21, 2007, pp. 2682-2687.

[6] C. T. Wang and R. J. Willey, "Oxidation of Methanol over Iron Oxide Based Aerogels in Supercritical CO_2," *Journal of Non-Crystalline Solids*, Vol. 225, 1998, pp. 173-177. http://dx.doi.org/10.1016/S0022-3093(98)00040-4

[7] S. Al-Sayari, A. F. Carley, S. H. Taylor and G. J. Hutchings, "Au/ZnO and Au/Fe_2O_3 Catalysts for CO Oxidation at Ambient Temperature: Comments on the Effect of Synthesis Conditions on the Preparation of High Activity Catalysts Prepared by Coprecipitation," *Topics in Catalysis*, Vol. 44, No. 1-2, 2007, pp. 123-128. http://dx.doi.org/10.1007/s11244-007-0285-9

[8] Y. Wang and B. H. Davis, "Fischer-Tropsch Synthesis. Conversion of Alcohols over Iron Oxide and Iron Carbide Catalysts," *Applied Catalysis A*: *General*, Vol. 180, No. 1-2, 1999, pp. 277-285. http://dx.doi.org/10.1016/j.apcatb.2005.10.039

[9] F. M. Bautista, J. M. Campelo, D. Luna, J. M. Marinas, R. A. Quiros and A. A. Romero, "Screening of Amorphous Metal-Phosphate Catalysts for the Oxidative Dehydrogenation of Ethylbenzene to Styrene," *Applied Catalysis B*: *Environmental*, Vol. 70, No. 1-4, 2007, pp. 611-620. http://dx.doi.org/10.1016/j.apcatb.2005.10.039

[10] V. R. Pradhan, D. E. Herrick, J. W. Tierney and I. Wender, "Finely Dispersed Iron, Iron-Molybdenum, and Sulfated Iron Oxides as Catalysts for Coprocessing Reactions," *Energy & Fuels*, Vol. 5, No. 5, 1991, pp. 712-720. http://dx.doi.org/10.1021/ef00029a015

[11] V R. Pradhan, J. Hu, J. W. Tierney and I. Wender, "Activity and Characterization of Anion-Modified Iron(III) Oxides as Catalysts for Direct Liquefaction of Low Pyrite Coals," *Energy & Fuel*, Vol. 7, No. 4, 1993, pp. 446-454. http://dx.doi.org/10.1021/ef00040a002

[12] G. T. Hager, E. N. Givens and F. J. Derbyshire, "The Activity of Nanoscale Iron Oxide for Model Compounds Reactions," *ACS-Division of Fuel Chemistry Preprints*, Vol. 38, 1993, pp. 1087-1096.

[13] Z. Zhong, J. Ho, J. Teo, S. Shen and A. Gedanken, "Synthesis of Porous Alpha-Fe$_2$O$_3$ Nanorods and Deposition of Very Small Gold Particles in the Pores for Catalytic Oxidation of CO," *Chemistry of Materials*, Vol. 19, No. 19, 2007, pp. 4776-4780. http://dx.doi.org/10.1021/cm071165a

[14] A. K. Kandalam, B. Chatterjee, S N. Khanna, B. K. Rao, P. Jena and B. V. Reddy, "Oxidation of CO on Fe$_2$O$_3$ Model Surfaces," *Surface Science*, Vol. 601, No. 21, 2007, pp. 4873-4880. http://dx.doi.org/10.1016/j.susc.2007.08.015

[15] H. Martin, H. Pavla and P. Jiri, "Quasi-Isothermal Decomposition: A Way to Nanocrystallinemesoporous Like Fe$_2$O$_3$ Catalyst for Rapid Heterogeneous Decomposition of Hydrogen Peroxide," *Journal of Materials Chemistry*, Vol. 20, 2010, pp. 3709-3715. http://dx.doi.org/10.1039/c000632g

[16] T. L. Jorgensen, H. Livbjerg and P. Glarborg, "Homogeneous and Heterogeneously Catalyzed Oxidation of SO$_2$," *Chemical Engineering Science*, Vol. 62, No. 16, 2007, pp. 4496-4499. http://dx.doi.org/10.1016/j.ces.2007.05.016

[17] M. L. Peterson, J. G. E. Brown, G. A. Parks and C. L. Stein, "Differential Redox and Sorption of Cr(III/VI) on Natural Silicate and Oxide Minerals: EXAFS and XANES Results," *Geochimica et Cosmochimica Acta*, Vol. 61, No. 16, 1997, pp. 3399-3412. http://dx.doi.org/10.1016/S0016-7037(97)00165-8

[18] S. Zhou, M. Johnson and J. G. C. Veinot, "Iron/Iron Oxide Nanoparticles: A Versatile Support for Catalytic Metals and Their Application in Suzuki-Miyaura Cross-Coupling Reactions," *Chemical Communications*, Vol. 46, No. 14, 2010, pp. 2411-2413. http://dx.doi.org/10.1039/b922462a

[19] M. Ilyas and M. Sadiq, "Liquid Phase Aerobic Oxidation of Benzyl Alcohol Catalyzed by Pt/ZrO$_2$," *Chemical Communications*, Vol. 30, No. 10, 2007, pp. 1391-1397. http://dx.doi.org/10.1002/ceat.200700072

[20] Y. P. Ji, G. O. Seong and H. H. Baik, "Characterization of Imn01I) Oxide Nanoparticles Prepared Ammonium Acetate as Precipitating Agent," *Korean Journal of Chemical Engineering*, Vol. 18, 2001, pp. 215-219.

[21] W. Damien, D. Olivier, P. Fabrice and A. Denis, "Alaboratory Study of the Reduction of Iron Oxides," In: F. Kongoli and R. G. Reddy, Eds., *Proceedings of Hydrogensohn International Symposium*, San Diego, 27-31 August 2006, p. 111.

[22] H. E. Ghandoor, H. M. Zidan, M. M. H. Khalil and M. I. M. Ismail, "Synthesis and Some Physical Properties of Magnetite (Fe$_3$O$_4$) Nanoparticles," *International Journal of Electrochemical Science*, Vol. 7, 2012, pp. 5734-5745.

[23] D. M. Sherman and T. D. Waite, "Electronic Spectra of Fe^{3+} Oxides and Oxide Hydroxides in the near IR to near UV," *American Mineralogist*, Vol. 70, 1985, pp. 1262-1269.

[24] H. Jung, H. Park, J. Kim, J. H. Lee, H. G. Hur, N. V. Myung and H. Choi, "Preparation of Biotic and Abiotic Iron Oxide Nanoparticles (IOnPs) and Their Properties and Applications in Heterogeneous Catalytic Oxidation," *Environmental Science & Technology*, Vol. 41, No. 13, 2007, pp. 4741-4747. http://dx.doi.org/10.1021/es0702768

[25] S. T. Amyn and K. Pei-Yoong, "Synthesis, Properties, and Application of Magnetic Iron Oxide Nanoparticles," *Progress in Crystal Growth and Characterization of Materials*, Vol. 55, No. 1-2, 2009, pp. 22-45. http://dx.doi.org/10.1016/j.pcrysgrow.2008.08.003

[26] S. M. Chaudhari, A. S. Waghulde, V. Samuel, M. L. Bari and V. R. Chumbhale, "Characterization of ZnO and Modified ZnO Catalysts for Anaerobic Oxidation of Cyclohexanol," *Research Journal of Chemical Sciences*, Vol. 3, 2013, pp. 38-44.

[27] H. I. Rekkab, B. A. Choukchou, R. L. Pirault and C. Kappenstein, "Catalytic Oxidation of Cyclohexane to Cyclohexanone and Cyclohexanol by Tert-Butyl Hydroperoxide over Pt/Oxide Catalysts," *Bulletin of Materials Science*, Vol. 34, No. 5, 2011, pp. 1127-1135. http://dx.doi.org/10.1007/s12034-011-0157-6

[28] M. Dominique and D. Daniel, "Evaluation of the Acid-Base Surface Properties of Several Oxides and Supported Metal Catalysts by Means of Model Reactions," *Journal of Molecular Catalysis A*: *Chemical*, Vol. 118, No. 1, 1997, pp. 113-128. http://dx.doi.org/10.1016/S1381-1169(96)00371-8

[29] F. M. Bautista, J. M. Campelo, A. Garcia, D. Luna, J. M. Marinas, R. A. Quiros and A. A. Romero, "Influence of Acid-Base Properties of Catalysts in the Gas-Phase Dehydration-Dehydrogenation of Cyclohexanol on Amorphous AlPO$_4$ and Several Inorganic Solids," *Applied Catalysis A*: *General*, Vol. 243, No. 1, 2003, pp. 93-107. http://dx.doi.org/10.1016/S0926-860X(02)00540-9